

Article

Durability Study of Frequent Dry–Wet Cycle on Proton Exchange Membrane Fuel Cell

Dan Wang^{1,2}, Haitao Min¹, Weiyi Sun^{1,*}, Bin Zeng² and Haiwen Wu³¹ State Key Laboratory of Automotive Simulation and Control, Jilin University, Changchun 130022, China² Xiangyang Da'an Automobile Test Center Limited Corporation, Xiangyang 441022, China³ China Certification & Accreditation Institute, Beijing 100011, China

* Correspondence: swy_18@jlu.edu.cn

Abstract: Durability is the key issue for the proton exchange membrane fuel cell application and its commercialization. Current research usually uses the accelerated stress test to decrease the experiment time, whereas the performance evolution—especially the internal state evolution—under real use may be different from that under the accelerated stress test. In addition, studies rarely report this kind of durability in real decay scenarios. This paper investigates the seldom-reported impact of dry–wet cycles on durability in terms of open circuit voltage (OCV), inner resistance, and hydrogen crossover current at the condition of 20,000 cycles or the equivalent 400 h, while simultaneously running the test for the same time interval in the control experiment. The mechanical and chemical test is independent. Frequent dry–wet cycles make the OCV decay over 14% compared to 6.9% under the normal decay. Meanwhile, the dry–wet cycle helps to alleviate deterioration in terms of the inner resistance decline (61% vs. 37%) and in terms of the hydrogen crossover current increase (−64% vs. 15%). The inner state evolution is irregular and against common sense. The relationship between the crack, platinum transfer, and the moisture which heals the crack is the potential reason for the above-mentioned phenomena. These findings are beneficial to navigating fuel cell storage.

Keywords: PEMFC; lifetime prediction; durability control

Citation: Wang, D.; Min, H.; Sun, W.; Zeng, B.; Wu, H. Durability Study of Frequent Dry–Wet Cycle on Proton Exchange Membrane Fuel Cell. *Energies* **2023**, *16*, 4284. <https://doi.org/10.3390/en16114284>

Academic Editors: Antonino S. Aricò and Daniel T. Hallinan Jr.

Received: 19 February 2023

Revised: 3 April 2023

Accepted: 20 April 2023

Published: 24 May 2023



Copyright: © 2023 by the authors. Licensee MDPI, Basel, Switzerland. This article is an open access article distributed under the terms and conditions of the Creative Commons Attribution (CC BY) license (<https://creativecommons.org/licenses/by/4.0/>).

1. Introduction

Although large-scale utilization of renewable energy is inevitable, the unique intermittence and instability of renewable energy have brought major challenges to the stable operation of the power system, opening temporal and spatial gaps between the consumption of the energy by end-users and its availability [1]. Obviously, PEMFC (Proton Exchange Membrane Fuel Cell) directly convert chemical energy into electricity, and are not restricted by the Carnot cycle, so the energy conversion efficiency is high, PEMFC does not face these issues; it can be an effective means of achieving stable and efficient energy generation. With the commercialization of the proton exchange membrane (PEM) fuel cell (PEMFC) [2], lowering the cost and prolonging the service lifetime are becoming the prominent issues. In the demonstration operation of fuel cell vehicles, it is found that the main bottleneck in the development of fuel cell city buses is the service life of fuel cell packs. In bench tests, the service life of single fuel cell is more competitive than that of traditional internal combustion engine. In case of decreasing the platinum loading to lower the cost, the lifetime of the fuel cell should not obviously decline. The key to solving the above issues is the investigation of the durability, which always involves the degradation mechanism of the materials and the lifetime prediction of the PEMFC [3].

On the degradation mechanism, the membrane electrolyte assembly is investigated. For the PEM, the mechanical degradation caused by the mechanical and fatigue [4], the thermal degradation caused by the thermal load [5], and the chemical degradation caused by the harmful byproduct of the electrochemical reaction [6] are the three main factors

affecting the degradation, which usually leads to the increase of hydrogen crossover current. For the platinum, the platinum dissolution [7], the carbon corrosion, the Ostwald ripening [8], agglomeration and particle detachment are the main factors which will lead to the decrease of the electrochemical active specific surface area. It is common sense that the high potential will aggravate the platinum degradation.

For the commercialization of the PEMFC, the operating conditions' impact on the degradation is the more meaningful avenue of research. Takahashi et al. [9] investigated the impact of cold start cycling on the durability and found that cold start cycling of $-30\text{ }^{\circ}\text{C}$ will lead to the thinning of the cathode layer up to 13%, and that the formation of ice will cause the high internal voltage and cathode carbon corrosion. Hara et al. [10] studied the impact of start/stop on durability via the voltage step cycle test and found that the catalyst durability was dependent on the average size and dispersion state of the platinum particles, and the platinum/graphitized carbon black catalysts were clearly detected. Wang et al. [11] investigated the impact of idling-rated-current cycles on degradation through high-frequency resistance and surface morphology characterization and found that the degradation occurs at both idling and rated current operations, where the former caused degradation of $1.0\text{ }\mu\text{V cycle}^{-1}$ while the latter caused degradation of $2.0\text{ }\mu\text{V cycle}^{-1}$.

The optimization of durability, durability control and life prediction of PEMFC restrict the industrialization application of PEMFC. On durability control, studies aim to find some ways to prevent the PEMFC from rapid lifetime decay. Liu et al. [12] proposed a cathode recirculation control to control the oxygen partial pressure from long-time high potential. Eskin and Yesilyurt [13] proposed an anode bleeding method via ultra-low flow rate to avoid severe voltage transients and a detrimental platinum-active surface area, where a super-high hydrogen utilization rate of 99.88% could be realized. Li et al. [14] put forward the attempt from the perspective of system device control, such as with respect to an air compressor. Apart from active control, many researchers implemented the durability improvement from the perspective of material design. Lopicque et al. [15] gave some ways to promote the durability of the micro porous layer and the gas diffusion layer, such as the deposition of the porous titanium design, adding antimony-doped tin oxide to conventional Vulcan XC-72, and the silicon carbide based micro porous layer, etc. Sun et al. [16] synthesized a Nafion-stabilized platinum nanoparticle colloidal solution through ethylene glycol reduction to enhance durability. Gomez et al. [17] presented an electrospray technique to fabricate the nanostructured electrode and used the addition of epoxy/graphene to the catalytic ink to improve durability. On the lifetime prediction, Chen et al. [18] proposed a novel extraction method of working condition spectrum for the lifetime prediction and energy management strategy evaluation of automotive fuel cells. Li et al. [19] gave a recognition prediction method for predicting and controlling the lifetime of the fuel cell hybrid bus. Numerical methods are another way to conduct degradation research in terms of water transport [20] and vehicle use [21].

The concern for degradation research is that the test could not reflect the real decay. It should be noted that most of the degradation research uses the accelerated stress test [22] so as to decrease the test time tremendously. Wan [23] studied the durability using the accelerated stress test and found $48\text{ }\mu\text{V h}^{-1}$'s degradation after 850 h of operation. Zhao et al. [24] investigated the degradation under a short number of dry-wet cycles. Ishikawa et al. [25] studied the degradation of a new gas diffusion layer material under wet-dry cycles. However, the specific decay under the accelerated stress test is not always the same as that under normal usage. More importantly, the research on the degradation under normal usage is limited. There are only a few papers undertaking this kind of research. Hence, the real decay mechanism may be different from that under the accelerated stress test. Vichard et al. [26] conducted a real 5000 h test in an open cathode fuel cell system and found that the performance loss was lower than 10%. Nevertheless, the test of the real usage under other operating conditions is rarely reported; meanwhile, the inner state evolution through this process also needs to be investigated.

This paper studies the attenuation mechanism of fuel cells under normal dry and wet cycling. Although the current proton exchange membrane is very thin, the manufacturer has optimized the structure, and the mechanical strength is not necessarily worse than that of the thick membrane. The membrane is very sensitive to humidity, and humidity cycling will lead to the swelling and shrinking cycle of the membrane. In the battery, this kind of mechanical cycle can easily create a relatively large mechanical pull where the membrane is connected to the frame, and as membranes used are very thin, it is easy to damage the structure of the membrane, resulting in air leakage at the junction. In order to screen the membrane with better tolerance as the membrane electrode, we assembled the membrane into a battery for the cycle durability test. As it is closer to the actual use of the membrane state, testing the mechanical durability of the membrane through wet and dry cycles and testing the change of hydrogen osmosis current density before and after the cycle is of great significance for selecting the membrane electrode with better mechanical durability.

The impact of frequent dry–wet cycles on the durability for at least 400 h were studied, with the long-time open circuit operation as the control experiment for the same amount of time. The dry-wet atmosphere occurs at the plateau places where the humidity changes too much in a whole day and night. More importantly, the load changing will also lead to the humidity change in part. This paper amplifies this scenario to an apparent humidity difference so as to reflect the accelerated stress. The inner states, in terms of internal resistance and hydrogen crossover current, are simultaneously measured. The overall experimental data are valuable for the durability research and some findings that are against common sense are found.

2. Experiment

The G20 Automated Single Cell Fuel Cell Test Station was used to test the fuel cell. The turndown (max:min flow) of all Mass Flow Controllers (MFC) is 100:1, the anode automatic intermittent nitrogen purge when the test equipment is shut down and in emergency stop. The flow can be manually adjusted. The max anode flow of the MFC for H₂ is 2 NLPM, The max cathode flow of the MFC for Air/N₂ switchable is 5 NLPM. Automatic re-fill bubbler humidification modules on anode and cathode is up to 90C dew point. Automated humidifier bypass permits delivery of 5–10%RH gas directly to stack. Heater hose assemblies for stack connection is up to 110C inlet gas. The nitrogen purged on anode and cathode. Automatic back pressure control module is between 0 and 3 Bar. Stack end-plate heater is used PID control (2 × 1 A max-heaters to be supplied by customer). The power of electronic load bank is 650 W, The voltage is 50 V, the current is 125 A ±0.05%FS, the maximum current available down to 0.0 V was used. The range of one channel cell voltage monitor is ±5 V range, the accuracy is ±1 mV. H₂ gas detector (CE, ATEX, UL, CSA) was used to test station E-stop and warning. The G20 test station has a number of distinct advantages, including: Excellent pressure control at low flow rates with optional pressure controller (±2 kPa steady state; Automatic N₂ purge on shutdown with controlled duration; Numerous options including humidifier by-pass, additional gas inputs and impedance spectroscopy, etc.

The activation process before the durability test is as follows: (1) Give a fixed flow rate (0.5/0.5 L/min) first, and then give the temperature. While giving the temperature, give the load current (2.5 A–5 A–7.5 A–10 A), and always pay attention to the voltage being not lower than 0.5 V. When the temperature rises to 50–60 °C, give the outlet back pressure and increase it every 20 kPa. Note that the outlet pressure difference between the cathode and anode should not exceed 20–30 kPa. The inlet pressure and the inlet and outlet pressure differences are of no concern, please ignore; (2) When the back pressure reaches 150 kPa, the flow can be changed to the metering ratio mode (1.5/2.5); (3) When the pressure meets the requirements, the flow setting is completed, and the temperature reaches above 60 °C, the current load can be increased. Pay attention to the voltage not being too low. When the voltage reaches 0.5 V, be sure to switch to the constant voltage mode and keep the voltage at 0.51 V, activate for 1 h; (4) After the activation is completed, first reduce the load

to about 5 A, and then reduce the pressure stepwise (20 kPa section) until it meets the test requirements. Then, change the load, change the temperature, and change the flow.

The points for attention during activation test are as follows: (1) Since the cooling and heating of the test bench is slow, it is recommended that after the LSV test is completed, the temperature conditions should be changed and activated at the same time, without waiting for the temperature to reach the set value. Similarly, while purging with nitrogen, the temperature can also be raised; (2) Before the LSV test, H_2/N_2 must be purged to below 0.1 V, the flow rate shall not be higher than 0.8 L/min, and the flow rate must be reduced to 0.2 L/min when it is around 0.1 V; (3) It is recommended that experiments be conducted in this order: activation, working condition change, resistance at 0.2 A/cm² (working condition is the same as durability test), durability test, working condition change, nitrogen purge (temperature control can be performed at the same time), LSV test, working condition change, activation (temperature control can be performed at the same time), and cycle the above process.

The mechanical durability test and chemical durability test were conducted at a single fuel cell. The mechanical durability test (Figure 1a) was carried out under dry-wet cycles with the fuel cell maintained as the open circuit state. The test procedure is as follows:

- (1) Activate the battery (refer to the “Membrane Electrode Test and Evaluation System” for the activation method and stay at the rated operating point for more than 2 h until the performance is stable). The activation procedure is the same as above;
- (2) Cycle test: 0%RH (30 s)~90 °C dew point (45 s) (normal temperature dry gas (30 s)~90 °C humidity (45 s));
- (3) Conduct air permeability current (LSV) and high-frequency impedance (EIS) tests at 0.2 A/cm² every 50 h, where LSV should be performed at 80 °C, 100% humidified, and without back pressure;
- (4) The experiment stops when the OCV decreases by 20%; or the LSV value is ≥ 15 mA/cm²; or the experiment stops when 20,000 cycles are completed.

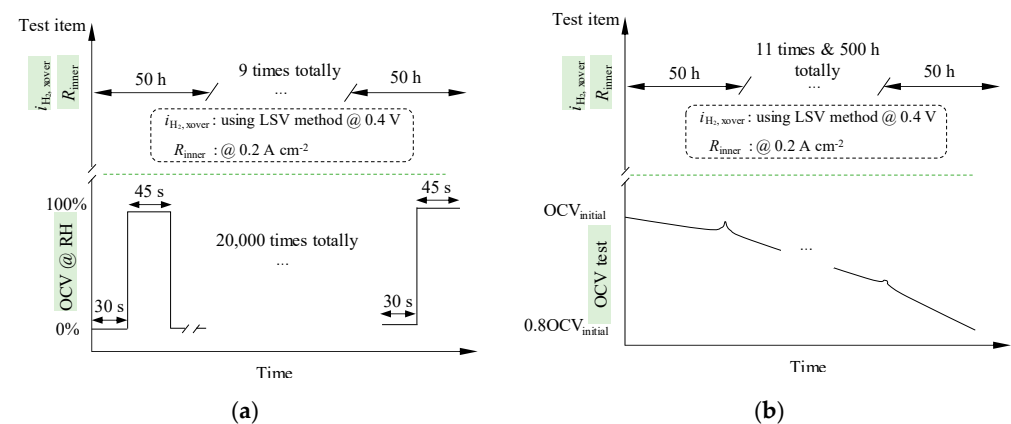


Figure 1. Experimental method: (a) mechanical durability test; (b) chemical durability test.

- (1) Similarly, the chemical durability test (Figure 1b) was carried out under open circuit state until the open circuit voltage (OCV) declines 20%, during which, the $i_{H_2,over}$ and the inner resistance was measured for every 50 h in the same conditions in which they were measured in the mechanical durability test. The test procedure is as follows: Activate the battery (refer to the “Membrane Electrode Test and Evaluation System” for the activation method, and stay at the rated operating point for more than 1 h until the performance is stable);
- (2) After the activation is completed, keep the battery at the open circuit voltage (OCV) state, record the OCV change value until the OCV is reduced by 20%, and record the OCV running time (at least 500 h);

- (3) Conduct air permeability current (LSV) and resistance test at 0.2 A/cm^2 current density were tested every 50 h (be sure to blow H_2/N_2 until the voltage drops below 0.1 V) was tested. After activation, the resistance between the graphite plates was tested with a multimeter. The ohmic resistance between the plates was tested 3 times, and the data were recorded manually. LSV should be performed at $80 \text{ }^\circ\text{C}$, 100% humidified, and with no back pressure;
- (4) Test end point: OCV attenuation of 20%; or LSV value $\geq 15 \text{ mA/cm}^2$.

The test bench was exhibited as Figure 2. The parameters of the sample and the operating conditions are listed as Table 1, where the Gore catalyst-coated membrane is selected with the thickness of $12 \text{ }\mu\text{m}$ and area $50 \text{ mm} \times 50 \text{ mm}$ and the SGL carbon paper is selected. The experiment description was referred to in [27].



Figure 2. Experimental bench.

Table 1. Parameters of the sample and operating conditions.

(a) MEA chemical Stability and Metrics (Test Using an MEA)			
Test condition	Steady-state OCV, single cell		
Sample	Catalyst coated membrane from Gore with $12 \text{ }\mu\text{m}$ thickness, and $50 \text{ mm} \times 50 \text{ mm}$ area. Carbon paper from SGL.		
Test bench	Test system from Green Light, Canada. Electrochemical workstation from Gamry.		
Total time	500 h		
Fuel cell operating temperature	$80 \text{ }^\circ\text{C}$		
Anodic/cathodic flow rate:	1.5/4.0 SLPM		
Relative humidity	Anode/cathode 30/30%		
Fuel/oxidant	H_2/air at stoics of 10/10 at 0.2 A/cm^2 equivalent flow; 99.999% H_2		
Pressure, outlet kPa abs	Anode/cathode 150/150 kPa		
Metric	Frequency	Target	
F-release or equivalent for nonfluorinated membranes	At least every 24 h	No target-for monitoring	
Hydrogen crossover (mA/cm^2)	Every 24 h	$\leq 15 \text{ mA/cm}^2$	
OCV	Continuous	Initial OCV $\geq 0.95\text{V}$, $<20\%$ OCV decrease during test	
High-frequency resistance	Every 24 h at 0.2 A/cm^2	No target-for monitoring	
Shorting resistance	Every 24 h	$>1000 \text{ ohm cm}^2$	
(b) Membrane chemical/Mechanical Cycle and Metrics (Test Using an MEA)			
Sample	Catalyst coated membrane from Gore with $12 \text{ }\mu\text{m}$ thickness, and $50 \text{ mm} \times 50 \text{ mm}$ area. Carbon paper from SGL.		
Cycle	Cycle 0% RH (30 s) to $90 \text{ }^\circ\text{C}$ dew point (45 s), single cell		
Total time	Until crossover $> 15 \text{ mA/cm}^2$ or 20,000 cycles		
Fuel cell operating temperature	$80 \text{ }^\circ\text{C}$		
Relative humidity	Cycle from 0% RH (30 s) to $90 \text{ }^\circ\text{C}$ dew point (45 s)		
Fuel/oxidant	H_2/air at 40 sccm/cm^2 on both sides; 99.999% H_2		
Pressure	Ambient or no back pressure		
Metric	Frequency	Target	
F-release or equivalent for nonfluorine membranes	At least every 24 h	No target-for monitoring	
Hydrogen crossover (mA/cm^2)	Every 24 h	$\leq 15 \text{ mA/cm}^2$	
OCV	Continuous	Initial wet OCV $\geq 0.95\text{V}$, $<20\%$ OCV decrease during test	
High-frequency resistance	Every 24 h at 0.2 A/cm^2	No target-for monitoring	
Shorting resistance	Every 24 h	$>1000 \text{ ohm cm}^2$	

3. Results and Discussion

3.1. General Influence for Durability

Figure 3 demonstrates the initial and final state of the tested fuel cell after 20,000 dry–wet cycles (~450 h) for the mechanical durability test and long-time high potential for ~500 h for the chemical durability test, respectively. In the mechanical durability test, the OCV declined from 0.986 V to 0.846 V, the inner resistance decreased from 43.09 Ω to 16.66 Ω , and the $i_{H_2, \text{crossover}}$ declined from 5.24 to 1.86 mA cm^{-2} . In the chemical durability test, the three variables evolve from 0.984 V, 62.43 Ω , and 2.8 mA cm^{-2} to 0.916 V, 39.21 Ω , and 3.21 mA cm^{-2} , respectively.

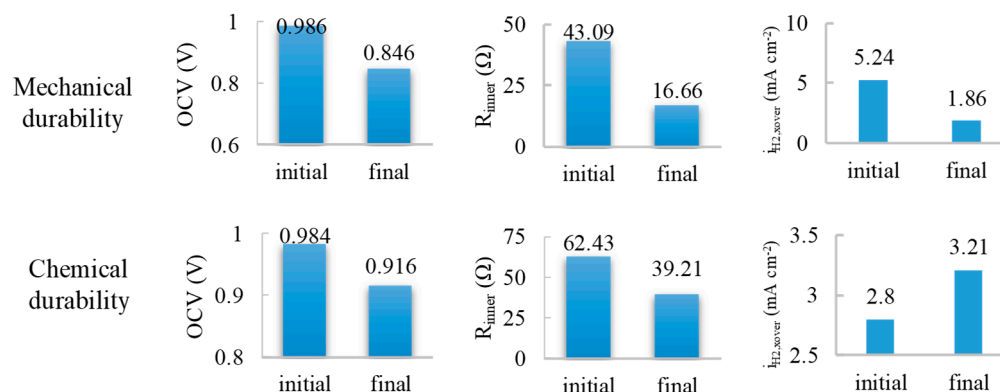


Figure 3. The initial and final state in terms of OCV, inner resistance, and hydrogen crossover current in the durability tests.

Although the fuel cell is maintained to the open circuit state in both tests, the 20,000 dry–wet cycles cause more remarkable changes. Alternating inlet humidity, resulting in an extra mechanical crack in the CCM, coupled with a long-time high potential, leads to the prominent decline of the OCV. The decrease of inner resistance is because the slow humidification of the inlet air and hydrogen originated from the frequent dry–wet cycle, which can be equivalently regarded as an effective activation for the fuel cell. Unexpectedly, the hydrogen crossover current decreases as well. This could be attributed to the recovery effect triggered by the moisture against the extension of the crack.

The trend of the CCM state in the chemical durability test conforms to the expectation represented by the decrease in OCV and inner resistance, as well as the ramp-up of $i_{H_2, \text{crossover}}$ when the CCM is under high potential for almost 500 h.

The only difference between the mechanical and chemical durability test is the dry–wet cycle. Given that the total running time is almost the same (~450 h for the mechanical and test; ~500 h for the chemical durability test), it can be concluded that the frequent dry–wet cycle plays a significant role in OCV declining (14% vs. 6.9%). In addition, the CCM state deterioration is alleviated due to the frequent dry–wet cycle (61% vs. 37% in inner resistance decline); for the hydrogen crossover current in particular, it improves.

3.2. Dry–Wet Cycle Causing Mechanical Damage

Figures 4–6 are the specific evolution of OCV, inner resistance, and $i_{H_2, \text{crossover}}$ during the 20,000 dry–wet cycles. The changes of OCV, internal resistance, and $i_{H_2, \text{crossover}}$ with cycle number correspond to the blue curve. The OCV degradation could be divided into reversible and irreversible degradation. The OCV exhibits decline–increase–decline when eliminating the effect of the short-time close circuit—which demonstrates the reversible degradation—for the resistance and crossover current test. After ~5000 cycles, the OCV reaches the first valley of 0.9 V; whereas, trapped in the second valley of under 0.9 V after ~19,000 cycles, between them is the peak of ~0.93 V after ~10,000 cycles. Correspondingly, the inner resistance experiences the same evolution trend, as does $i_{H_2, \text{crossover}}$, whereas the first valley arrives early at about 3000th cycle.

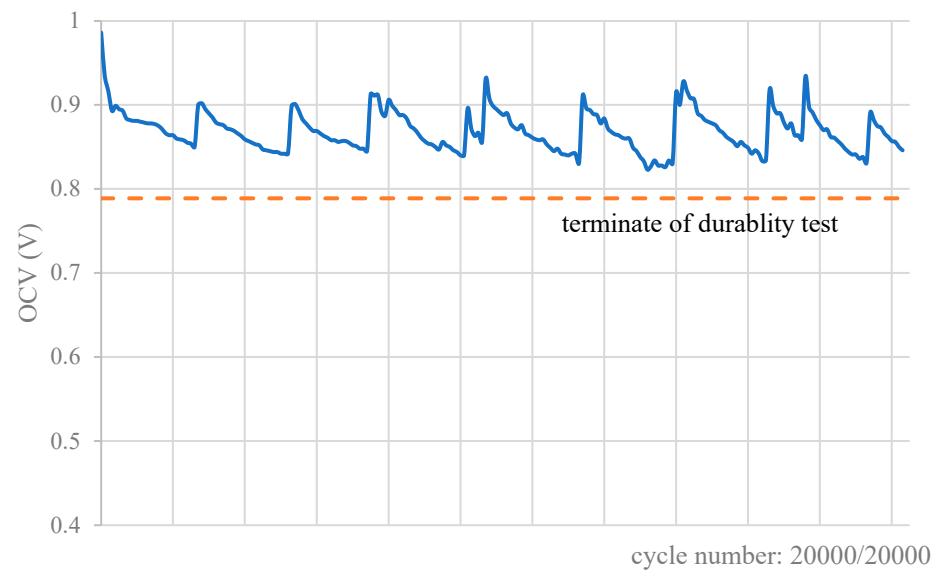


Figure 4. The OCV evolution during 20,000 dry–wet cycles.

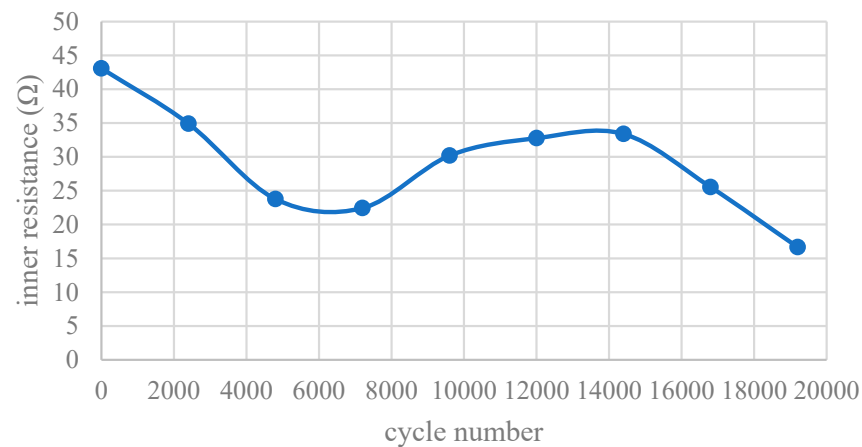


Figure 5. Inner resistance evolution in 20,000 dry–wet cycles.

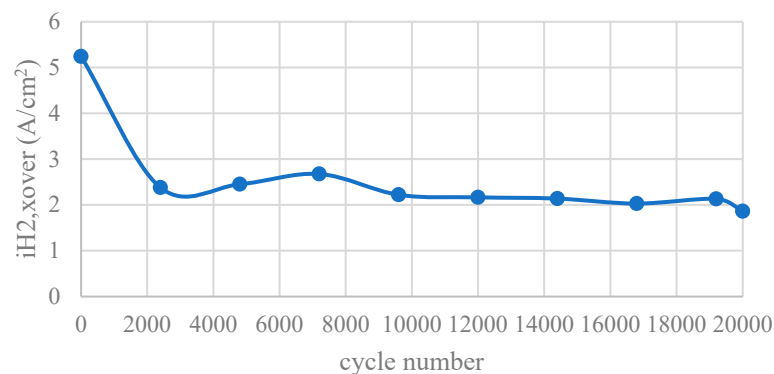


Figure 6. The evolution of $i_{H_2, xover}$ in 20,000 dry–wet cycles.

In particular, the OCV evolution is caused by three factors: (a) high potential, generating the catalyst degradation; (b) dry–wet cycles, causing the CCM crack, although the crack is alleviated due to the moisture supply; and (c) the platinum transfer towards the proton exchange membrane. These three factors play the main role in OCV's three stages (decline—increase—decline).

The first decline of inner resistance is caused by the moisture introduction. The ramp-up is caused by the emergence of the crack. The long-time plateau of the $i_{H_2, \text{crossover}}$ after 10,000 cycles is mainly because of the healing of the crack bridged by the moisture.

3.3. Typical Long-Time High Potential Affecting Durability

The change of OCV with time corresponds to the blue curve in Figure 7. As stated in 3.1, the prominent decline of the OCV (Figure 7) is due to the long-time high potential leading to catalyst degradation. The decline of inner resistance between 0~350 h in Figure 8 is because of the short-time discharging at 0.2 A cm^{-2} every 50 h, which could be regarded as an activation process; hence, proton transfer could be brought through after the short-time discharge. In addition, the degradation of catalysts before discharging could be rearranged by this kind of activation.

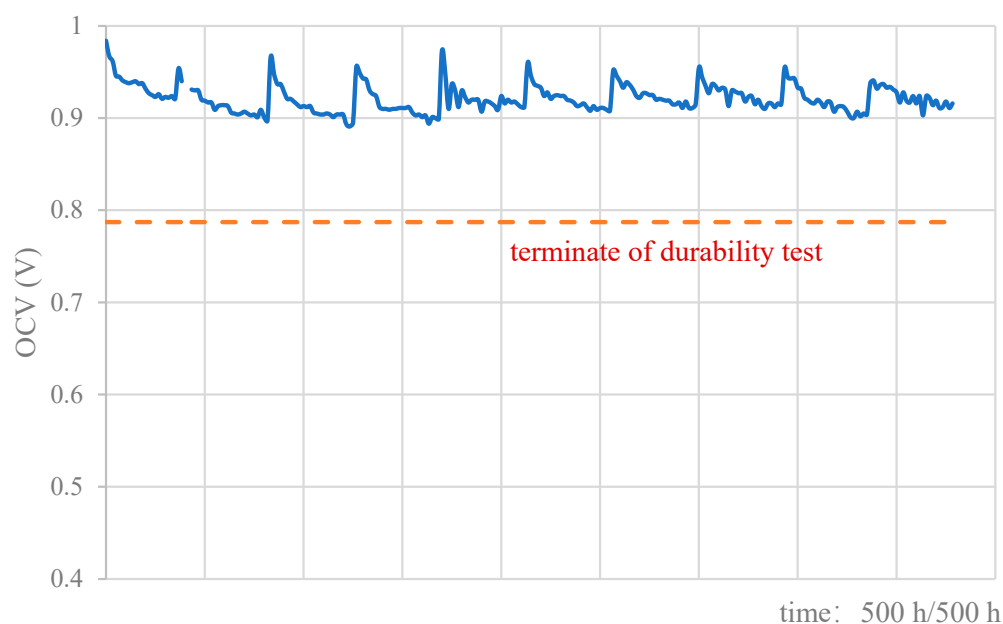


Figure 7. The OCV evolution in the chemical durability test.

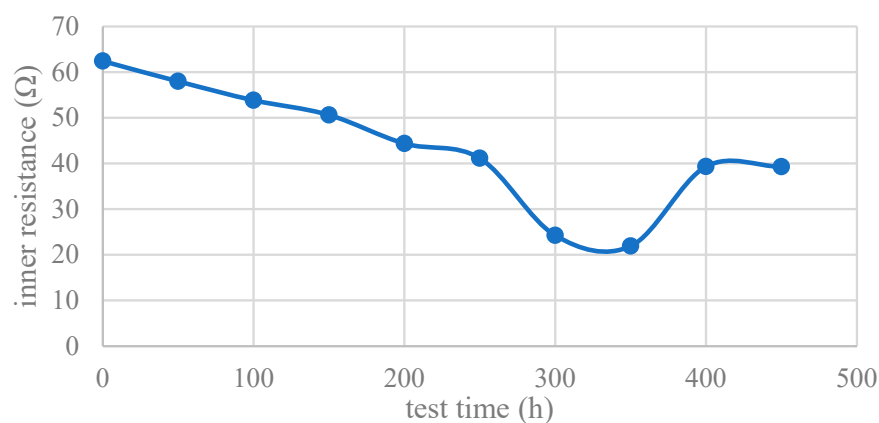


Figure 8. The inner resistance evolution in the chemical durability test.

The change of $i_{H_2, \text{crossover}}$ with time corresponds to the blue curve in Figure 9. The hydrogen crossover current increases during the first 50 h, then it maintains a steady value. The valley at the 250th h is a dead pixel produced by a logging error. It maintains a steady value from 300 h to 500 h. The increase in the first 50 h is caused by catalyst degradation. The slight decline and the plateau after 50 h are due to the build-up of the relative humidity at the catalyst surface, resulting from the discharging and water generation.

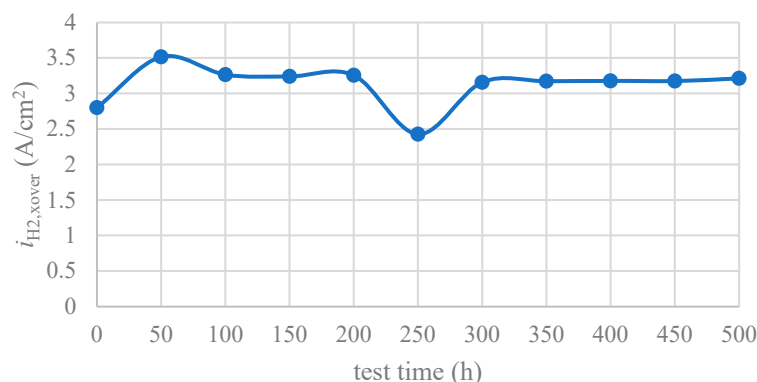


Figure 9. The evolution of $i_{H_2, crossover}$ in the chemical durability test.

4. Conclusions

The long-time storage of the proton exchange membrane fuel cell faces many problems such as the high potential issue and, in particular, the environment changing issue. This paper investigates the durability at different relative humidities in the form of dry–wet cycles, with the long-time high potential storage running as the control group. The cycle number is as high as 20,000, and the total operating time is more than 400 h. The experiment is representative. Some conclusions are listed as the following.

1. Compared to the pure high potential storage, the frequent dry–wet cycle plays a significant role in deteriorating the fuel cell open circuit voltage as much as 14%. However, the degradation of the catalyst coated membrane (CCM) is alleviated under the dry–wet cycle; for instance, the decline of inner resistance is as high as 61%, whereas it is 37% under pure high potential running. In addition, the hydrogen crossover current is improved, reflected by the declining $i_{H_2, crossover}$, whereas the value increases under the pure high potential running;
2. During the 20,000 dry–wet cycles, the CCM experiences catalyst degradation, crack, and platinum transfer towards the membrane;
3. The dry–wet cycles could also humidify the membrane, and, to some extent, the moisture could heal the crack so as to improve the activation effect;
4. From the perspective of open circuit voltage, we should avoid storing fuel cells at frequently changing humidities.

Author Contributions: Methodology, D.W., H.M. and H.W.; Software, D.W.; Formal analysis, D.W.; Investigation, H.M.; Resources, H.M.; Data curation, B.Z.; Writing—original draft, D.W.; Writing—review & editing, W.S.; Visualization, H.M. and W.S.; Supervision, H.M.; Project administration, W.S. and H.W. All authors have read and agreed to the published version of the manuscript.

Funding: The authors gratefully acknowledge the financial support from National Natural Science Foundation of China (Grant No. 5210245), the Special project of technical support for market supervision (2022YJ06), Major Science and Technology Projects in Jilin Province and Changchun City (20220301010GX).

Data Availability Statement: We welcome readers to email us to discuss the test data and research insights.

Conflicts of Interest: The authors declare no conflict of interest.

References

1. Zhang, H.; Sun, C.; Ge, M. Review of the Research Status of Cost-Effective Zinc–Iron Redox Flow Batteries. *Batteries* **2022**, *8*, 202. [[CrossRef](#)]
2. Li, Y.; Yang, F.; Chen, D.; Hu, S.; Xu, X. Thermal-physical modeling and parameter identification method for dynamic model with unmeasurable state in 10-kW scale proton exchange membrane fuel cell system. *Energy Convers. Manag.* **2023**, *276*, 116580. [[CrossRef](#)]

3. Li, B.; Wan, K.; Xie, M.; Chu, T.; Wang, X.; Li, X.; Yang, D.; Ming, P.; Zhang, C. Durability degradation mechanism and consistency analysis for proton exchange membrane fuel cell stack. *Appl. Energy* **2022**, *314*, 119020. [[CrossRef](#)]
4. Ren, P.; Pei, P.; Li, Y.; Wu, Z.; Chen, D.; Huang, S. Degradation mechanisms of proton exchange membrane fuel cell under typical automotive operating conditions. *Prog. Energy Combust. Sci.* **2020**, *80*, 100859. [[CrossRef](#)]
5. Guan, W.; Du, Z.; Wang, J.; Jiang, L.; Yang, J.; Zhou, X. Mechanisms of performance degradation induced by thermal cycling in solid oxide fuel cell stacks with flat-tube anode-supported cells based on double-sided cathodes. *Int. J. Hydrogen Energy* **2020**, *45*, 19840–19846. [[CrossRef](#)]
6. Wang, D.; Hu, J.; Liu, B.; Hou, H.; Yang, J.; Li, Y.; Zhu, Y.; Liang, S.; Xiao, K. Degradation of refractory organics in dual-cathode electro-Fenton using air-cathode for H₂O₂ electrogeneration and microbial fuel cell cathode for Fe²⁺ regeneration. *J. Hazard. Mater.* **2021**, *412*, 125269. [[CrossRef](#)]
7. Kovtunenkov, V.A.; Karpenko-Jereb, L. Study of voltage cycling conditions on Pt oxidation and dissolution in polymer electrolyte fuel cells. *J. Power Sources* **2021**, *493*, 229693. [[CrossRef](#)]
8. Okonkwo, P.; Ige, O.; Barhoumi, E.; Uzoma, P.; Abdullah, A. Platinum degradation mechanisms in proton exchange membrane fuel cell (PEMFC) system: A review. *Int. J. Hydrogen Energy* **2021**, *46*, 15850–15865. [[CrossRef](#)]
9. Takahashi, T.; Kokubo, Y.; Murata, K.; Hotaka, O.; Hasegawa, S.; Tachikawa, Y.; Nishihara, M.; Matsuda, J.; Kitahara, T.; Lyth, S.M.; et al. Cold start cycling durability of fuel cell stacks for commercial automotive applications. *Int. J. Hydrogen Energy* **2022**, *47*, 41111–41123. [[CrossRef](#)]
10. Hara, M.; Lee, M.; Liu, C.; Chen, B.; Yamashita, Y.; Uchida, M.; Uchida, H.; Watanabe, M. Electrochemical and Raman spectroscopic evaluation of Pt/graphitized carbon black catalyst durability for the start/stop operating condition of polymer electrolyte fuel cells. *Electrochim. Acta* **2012**, *70*, 171–181. [[CrossRef](#)]
11. Wang, G.; Huang, F.; Yu, Y.; Wen, S.; Tu, Z. Degradation behavior of a proton exchange membrane fuel cell stack under dynamic cycles between idling and rated condition. *Int. J. Hydrogen Energy* **2018**, *43*, 4471–4481. [[CrossRef](#)]
12. Liu, Z.; Xu, S.; Guo, S. High-potential control for durability improvement of the vehicle fuel cell system based on oxygen partial pressure regulation under low-load conditions. *Int. J. Hydrogen Energy* **2022**, *47*, 32607–32627. [[CrossRef](#)]
13. Eskin, M.G.; Yeşilyurt, S. Anode bleeding experiments to improve the performance and durability of proton exchange membrane fuel cells. *Int. J. Hydrogen Energy* **2019**, *44*, 11047–11056. [[CrossRef](#)]
14. Li, Y.; Pei, P.; Ma, Z.; Ren, P.; Huang, H. Analysis of air compression, progress of compressor and control for optimal energy efficiency in proton exchange membrane fuel cell. *Renew. Sustain. Energy Rev.* **2020**, *133*, 110304. [[CrossRef](#)]
15. Lapique, F.; Belhadj, M.; Bonnet, C.; Pauchet, J.; Thomas, Y. A critical review on gas diffusion micro and macroporous layers degradations for improved membrane fuel cell durability. *J. Power Sources* **2016**, *336*, 40–53. [[CrossRef](#)]
16. Sun, X.; Xu, H.; Zhu, Q.; Lu, L.; Zhao, H. Synthesis of Nafion®-stabilized Pt nanoparticles to improve the durability of proton exchange membrane fuel cell. *J. Energy Chem.* **2015**, *24*, 359–365. [[CrossRef](#)]
17. Gómez, M.A.; Navarro, A.J.; Giner-Casares, J.J.; Cano, M.; Fernández-Romero, A.J.; López-Cascales, J.J. Electrodes based on nafion and epoxy-graphene composites for improving the performance and durability of open cathode fuel cells, prepared by electrospray deposition. *Int. J. Hydrogen Energy* **2022**, *47*, 13980–13989. [[CrossRef](#)]
18. Chen, D.; Pei, P.; Meng, Y.; Ren, P.; Li, Y.; Wang, M.; Wang, X. Novel extraction method of working condition spectrum for the lifetime prediction and energy management strategy evaluation of automotive fuel cells. *Energy* **2022**, *255*, 124523. [[CrossRef](#)]
19. Li, J.; Yang, L.; Yang, Q.; Wei, Z.; He, Y.; Lan, H. Degradation adaptive energy management with a recognition-prediction method and lifetime competition-cooperation control for fuel cell hybrid bus. *Energy Convers. Manag.* **2022**, *271*, 116306. [[CrossRef](#)]
20. Um, S.; Wang, C.Y. Computational study of water transport in proton exchange membrane fuel cells. *J. Power Sources* **2005**, *156*, 211–223. [[CrossRef](#)]
21. Darvishi, Y.; Hassan-Beygi, S.R.; Zarafshan, P.; Hooshyari, K.; Malaga-Toboła, U.; Gancarz, M. Numerical Modeling and Evaluation of PEM Used for Fuel Cell Vehicles. *Materials* **2021**, *14*, 7907. [[CrossRef](#)] [[PubMed](#)]
22. Osmieri, L.; Cullen, D.A.; Chung, H.T.; Ahluwalia, R.K.; Neyerlin, K.C. Durability evaluation of a Fe–N–C catalyst in polymer electrolyte fuel cell environment via accelerated stress tests. *Nano Energy* **2020**, *78*, 105209. [[CrossRef](#)]
23. Wan, N. Durability study of direct methanol fuel cell under accelerated stress test. *J. Power Sources* **2023**, *556*, 232470. [[CrossRef](#)]
24. Zhao, J.; Shahgaldi, S.; Li, X.; Liu, Z.S. Experimental Observations of Microstructure Changes in the Catalyst Layers of Proton Exchange Membrane Fuel Cells under Wet-Dry Cycles. *J. Electrochem. Soc.* **2018**, *165*, F3337. [[CrossRef](#)]
25. Ishikawa, H.; Teramoto, T.; Ueyama, Y.; Sugawara, Y.; Sakiyama, Y.; Kusakabe, M.; Miyatake, K.; Uchida, M. Use of a sub-gasket and soft gas diffusion layer to mitigate mechanical degradation of a hydrocarbon membrane for polymer electrolyte fuel cells in wet-dry cycling. *J. Power Sources* **2016**, *325*, 35–41. [[CrossRef](#)]
26. Vichard, L.; Petrone, R.; Harel, F.; Ravey, A.; Venet, P.; Hissel, D. Long term durability test of open-cathode fuel cell system under actual operating conditions. *Energy Convers. Manag.* **2020**, *212*, 112813. [[CrossRef](#)]
27. Sabharwal, M.; Büchi, F.N.; Nagashima, S.; Marone, F.; Eller, J. Investigation of the transient freeze start behavior of polymer electrolyte fuel cells. *J. Power Sources* **2020**, *489*, 229447. [[CrossRef](#)]

Disclaimer/Publisher’s Note: The statements, opinions and data contained in all publications are solely those of the individual author(s) and contributor(s) and not of MDPI and/or the editor(s). MDPI and/or the editor(s) disclaim responsibility for any injury to people or property resulting from any ideas, methods, instructions or products referred to in the content.